Indian Journal of Pure & Applied Physics
Vol. 53, May 2015, pp. 320-327

Structural, spectral and thermal properties of bulky organic sulfonic acids doped polyanilines and antistatic performance of its melt blend

Parveen Saini[1]* & Veena Choudhary[2]

[1]Polymeric & Soft Materials Section, CSIR-National Physical Laboratory, New Delhi 110 012, India

[2]Centre for Polymer Science & Engineering, Indian Institute of Technology, New Delhi 110 016, India

*E-mail: pksaini@nplindia.org

Received 22 September 2014; revised 9 March 2015; accepted 1 April 2015

Aniline has been polymerized in the presence of dodecylbenzenesulfonic acid (DBSA), camphorsulfonic acid (CSA), ligninsulfonic acid (LSA) and cardanolazophenylsulfonic acid (CDSA) by emulsion route to form doped polyanilines (PANIs) designated as PDB, PCS, PLS and PCD, respectively. FTIR spectra and XRD patterns of samples confirm the formation of PANIs in doped emeraldine salt form. The UV-Visible spectra show that doping level increases in the order PCD<PLS<PCS<PDB which is in good agreement with electrical conductivity values. The TGA results show that all samples have thermal stability in excess of greater than 230°C which is more than the melt processing temperatures (T_p) of thermoplastics like low density polyethylene (LDPE, T_p~150-160°C) or polypropylene (PP, T_p~210-220°C), suggesting that these materials could be processed via melt blending route. It was observed that melt blended LDPE film containing 1.5 wt% PDB passes the antistatic criteria with static decay time <2 s.

Keywords: Conducting polymers, Polyaniline, Surfactant, Dopant, Sulfonic acid, Emulsion polymerization, Electrical conductivity, TGA, FTIR, UV-Visible Spectroscopy, XRD

1 Introduction

Organic conducting polymers and their composites are drawing enormous attention from scientific community due to their novel optical and electrical attributes[1-6]. Like the conventional inorganic semiconductors, these π-conjugated polymers can also be doped with different organic and inorganic moieties. However, here the doping level tends to be high (up to 50 mole %) so that even metallic conductivity can be realized, entitling them to be called as synthetic metals[3,5]. Depending on the nature and concentration of dopant, electrical conductivity can be precisely tuned to cater the need of a specific sector e.g. organic photovoltaic, organic light emitting diodes, sensors, electrochromic devices, electro-magnetic interference (EMI) shielding and electrostatic charge dissipation[1-15] (ESD). In particular, electrostatic dissipation (ESD) which is a critical issue especially with handling of sensitive electronic items (e.g. miniaturized electronic components, memory devices, integrated circuits, aviation/defense communication systems, medical instruments etc.) due to their susceptibility towards electrostatic discharge and consequent disturbance of performance or even complete breakdown[13,16,17].

As conventional polymers (that are widely used for packaging of electronic items) are electrically insulating in nature, they failed to dissipate any "tribo-electrically generated or contact electrification transferred" static charges. In principle, electrical conduction is the most important requirement for safe and rapid dissipation of static charges though the level of required conductivity is small[13,16]. Therefore, the electrical conductivity driven antistatic properties in conventional polymers e.g. by addition of antistatic agents[18], incorporation of conducting additives like metals or carbonaceous fillers[19-23], has been studied in the past. However, the functioning of antistatic agents is a function of humidity[24,25] whereas the metal and carbon filled materials suffered from the problems like bleeding, poor dispersion and irreproducible results[26]. In this context, conducting polymers with tunable conductivity and good processability can offer an attractive solution for safe drainage of static electricity[15,16]. Among various conducting polymers, polyaniline (PANI) has received enormous attention due to distinguished advantages like low monomer cost, facile synthesis, non-corrosiveness, good environmental/thermal stability and tunable electrical properties[4-10,15,16]. Chemically, polyaniline is composed of reduced (–B–NH–B–NH–) and oxidized (–B– N= Q= N–) repeated units where symbols 'B' and 'Q' denote benzenoid and quinoid forms of -C_6H_4-ring. These units are distributed along the

backbone so that the polyaniline can be represented by general structure $[(–B–NH–B–NH–)_y–(–B–N=Q=N–)_{(1-y)}]$, where '(1-*y*)' and '*n*' are oxidation state (OS) and degree of polymerization (DP), respectively. Therefore, depending on the oxidation state, different forms of polyaniline can be realized viz. leucoemeraldine (fully reduced, *y*=1), pernigraniline (fully oxidized, *y*=0) and emeraldine base (EB, 50% oxidized and 50 % reduced, *y*=0.5). The doping of EB with protonic acids covert it into emeraldine salt (ES) leading to formation of charge carriers i.e. polarons/bipolarons. However, even after doping, except ES all other forms are electrically insulating in nature which show that both oxidation state as well as protonic acid doping plays a critical role in determining the electrical properties of the polyaniline[27]. Though PANI can be made processable/soluble either by polymerizing functionalized anilines or by copolymerizing aniline with substituted monomers[6,14,15,28-30,] these routes often lead to measurable decrease in conductivity resulting in poor performance for applications where electrical properties are prime requisite. Further, the processability (via melt or solution phase) of PANI, which is a prime requisite for conversion into electrostatically useful product, is strictly governed by the nature and concentration of dopant[27,31-34]. Herein, we report the facile synthesis of doped yet processable polyanilines by in-situ polymerization of aniline in the presence of different bulky organic sulfonic acids which plays the dual role of surfactant as well as dopant. These samples were characterized by FTIR/UV-visible spectroscopy, XRD and TGA and results were compared to select the best dopant among DBSA, LSA, CSA and CDSA in terms of electrical conductivity and processability. Antistatic film was prepared by melt blending of PANI with low density polyethylene (LDPE) on a twin screw extruder followed by blown film extrusion, and the static charge decay test unit was used to assess its antistatic performance.

2 Experimental Details

Aniline (Loba Chemie, India) was freshly double distilled before use. The dodecyl benzene sulfonic acid (DBSA), camphor sulfonic acid (CSA), lignin sulfonic acid (LSA), cardanol azophenyl sulfonic acid (CDSA), ammonium persulfate (APS), ammonia (25% aqueous solution), isopropyl alcohol, chloroform were used as received basis. Aqueous solutions were prepared from the Millipore water of $>10^6$ ohm-cm resistivity value.

The doped polyaniline (PANI) that represents the conducting form was prepared by in-situ emulsion polymerization of aniline monomer in the presence of different "bulky counter-ion organic sulfonic acids" by procedure described elsewhere[35]. In a typical reaction, 0.3 mol dopant (DBSA, CSA, CARD, LSA) was homogenized with water (1.0 L) using high speed blender (rotating at ~10000 rpm) for about 30 min to uniformly disperse the phases to form an emulsion. 0.1 M aniline monomer was then added to above emulsion and blending continued for another 1 h. The reaction mixture was then transferred to double walled glass reactor and cooled to-5ºC under constant stirring. The polymerization was initiated by dropwise addition of 0.1 M aqueous solution of ammonium peroxydisulfate (APS) and the temperature was maintained at −5°C. After completion of polymerization (6 h), formed dark green emulsion was destabilized by adding copious amount of isopropyl alcohol. The stirring was continued for another 2 h after which the reaction mixture was filtered to separate the product. The wet polymer cake so obtained was vacuum dried and solid lumps were crushed to obtain the doped polyaniline powder. Four different polyaniline samples were prepared by taking DBSA, CSA, CARD and LSA as dopants and designated as PDB, PCS, PLS and PCD respectively.

Blending of conducting polymer or its filled composites with LDPE was done by melt blending route using a twin screw extruder (TSE, Prism Eurolab 16 XL, Thermo-Haake). During melt blending, 1.5 wt.% of PDB was taken and the extrusion was carried out at a screw speed of 60 rpm and keeping the temperature (of different zones) in the range 110-160°C. Finally, 80-120 μm thick films were prepared from above melt blends using a blown film extruder (BFE, Haake) operating at 130-160°C and at a screw speed of 40 rpm.

The FTIR spectra were recorded on Nicolet 5700 spectrometer. The UV-visible spectra were recorded in the 200-1100 nm wavelength range on chloroform solutions of doped PANI samples using Shimadzu 1601 spectrophotometer. The XRD patterns were recorded on Bruker-D8 advanced diffractometer using CuKα line (λ= 1.540598Å) as radiation source. The thermal stability was measured under inert atmosphere of flowing dry nitrogen gas (60 ml/min) using TGA (Mettler Toledo TGA/SDTA 851^e, Switzerland) system by taking 10±2 mg of sample inside an open platinum crucible. The materials were

heated from 25 to 800°C at a constant heating rate of 10°C/min.

3 Results and Discussion

The dopant brings significant changes in the properties of PANI because doping leads to protonation and involves ingress of "counter-anions" in the polymer matrix to maintain the electrical charge neutrality[3-5]. The nature and size of these counter-anions affect the properties e.g. they may increase or decrease the conductivity, solubility, compatibility or thermal/environmental stability of doped polymers[6,15,31,32,36,37]. The most important aspect of PANI synthesis is the pK_a value (i.e. negative logarithm of the acid dissociation constant K_a) of the acid, because in PANI protonation equilibria involve exclusively the quinone-diamine segment, having two imine nitrogen[38]with pK_{a1} = 1.05 and pK_{a2} = 2.55. So, any acid whose pK_a value falls in this range, would be suitable as a dopant. Similarly anilinium-ion has pK_a = 4.60 and the ammonium-ion has pK_a = 9.24. Thus, acids having pK_a value around that of an anilinium-ion would be suitable as a solvent if they are liquid or can also be used to restrict the over oxidation of aniline[4].

In overall terms, polymers represent a macromolecular system whose properties are strongly dependent upon the synthesis conditions (temperature, pressure or *p*H), reaction phase (solid, liquid, gas, homogenous or heterogeneous) and selected polymerization process[39] (bulk, solution, suspension or emulsion). In particular, the polymerization process influences the morphology; molecular weight; and purity of conducting polymers, which are the key attributes to electrical, optical and dielectric responses. In contrast to conventional bulk, solution or suspension polymerization techniques, emulsion polymerization has distinguished advantage of simultaneous maintenance of high polymerization rate as well as high molecular weight[40]. The side reactions like chain transfer leading to branched chain structures are effectively suppressed because the polymerization reaction is taking place inside in-situ formed tiny reactors known as micelles[41]. Such a strict control during emulsion polymerization results in quantitative yield of polymers. An amphiphilic molecule i.e. surfactant is the most important component of emulsion reaction[42]. These molecules consist of polar head and long non-polar tail e.g. non-polar dodecyl (i.e. $-C_{12}H_{25}$) and polar sulfonic-acid (i.e. $-SO_3H$) groups are responsible for amphiphilic nature of DBSA molecule. The "$-SO_3H$" group acts as a hydrophilic head, benzenoid (C_6H_4) segment act as spacer, whereas the "$-C_{12}H_{25}$" group constitutes a long hydrophobic tail, imparting surfactant characteristics to DBSA. Similarly, "$-SO_3H$" group acts as polar head whereas the remaining part of the dopant moiety (CDSA, CSA or LSA) acts as spacer and tail. Additionally, being a proton donor, "$-SO_3H$" group also impart dopant characteristic to these surfactants. Consequently, such molecules perform a dual function of surfactant as well as bulky organic dopant.

The surfactant in a liquid dispersion medium form aggregates (known as micelles) above critical miceller concentration[39-43] (CMC). The shape and size of micelles (spherical or elongated rod shape) are a function of the molecular geometry of surfactant, its concentration, nature of dispersion medium (aqueous/non-aqueous) as well as temperature, *p*H and ionic strength of the reaction system[39,40,44]. In aqueous (polar) medium, "oil-in-water" type micelles are formed[45] so that the hydrophilic "head" regions of the surfactant are in contact with surrounding dispersant (water), sequestering the hydrophobic tail regions towards non-polar micellar center. While, in non-aqueous (oily or non-polar) medium, inverted micelles ("water-in-oil" type) are formed with non-polar tail regions touching oily dispersant and polar heads forming the micellar centre. When dopant is dispersed in aqueous phase, oil in water type emulsion is formed where water constitutes the continuous phase and dopant aggregates (micelles) act discontinuous (oily) phase[46]. Addition of aniline (AN) monomer leads to the formation of dopant-AN charge transfer complex (Fig. 1), which assembled to form micelles[47]. Once the water soluble initiator (or oxidant) like APS is added, AN present at the micelle-water interface gets oxidized (initiation step) to form anilinium radical cations (Fig. 2) which subsequently combine with another unit to form neutral dimer[15,35,48-50]. Further, oxidation and coupling of this dimer lead to the formation of a termer and reaction continued likewise (chain propagation) to form the oligomers (tetramer, octamer etc.) and finally (after 6 h) a dark green colour dispersion of highly conducting doped PANI particles is formed. The competition between chain propagation termination/ chain transfers determines the properties. During the polymerization, the colour of the reaction mixture changes systematically from the initial

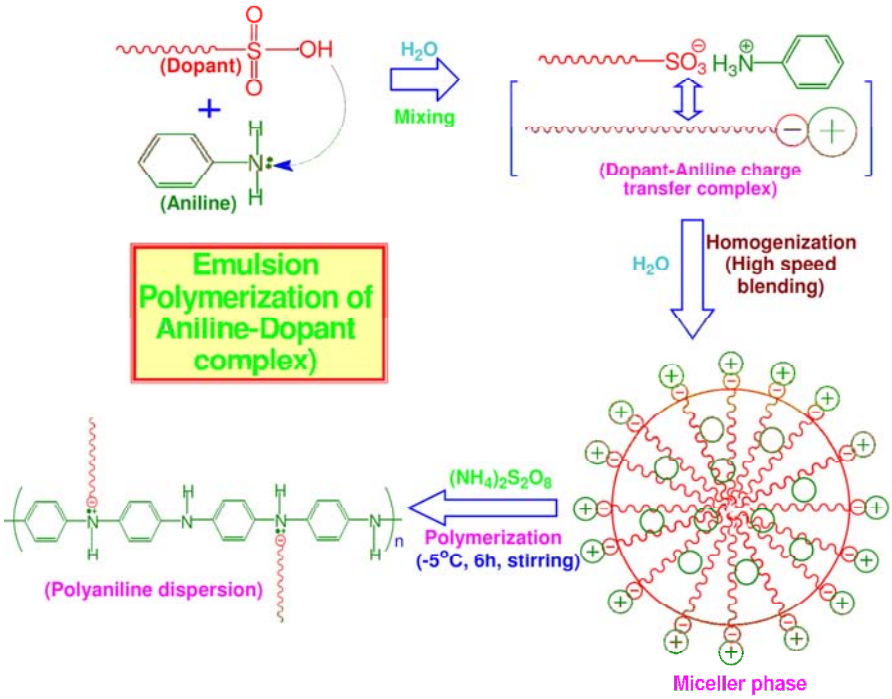

Fig. 1 — Schematic representation of in-situ emulsion polymerization of aniline in the presence of anionic surfactant dopants having sulfonic acid group

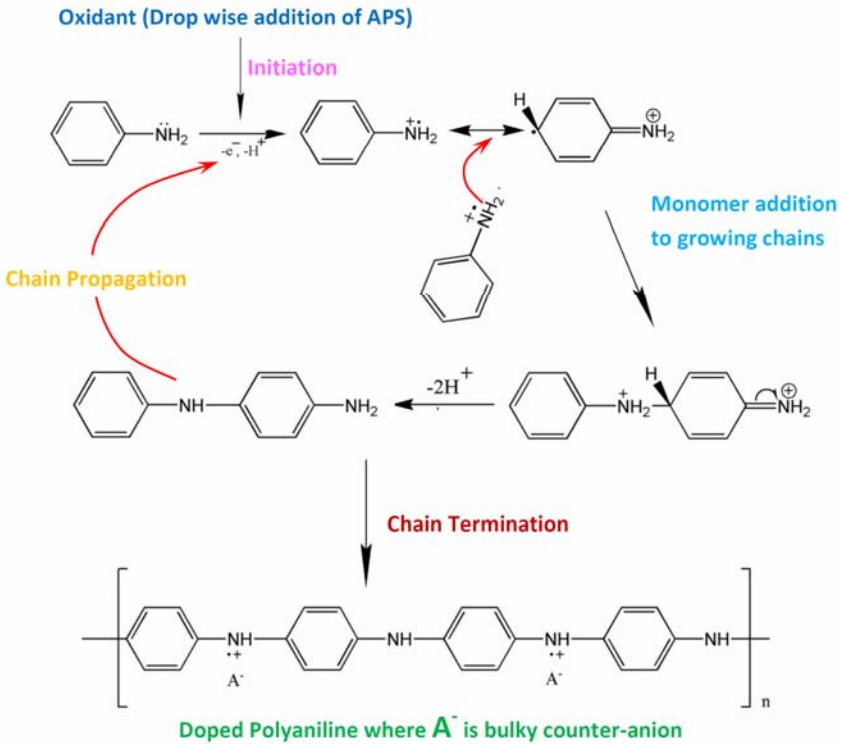

Fig. 2 — Schematic representation of chemical oxidative polymerization of aniline involving typical chain initiation, propagation and termination steps

pale-white→sea-green→dark-green. Generally, in micellar solution, there are the chances of formation of macroscopic particles (secondary growth) that can be prevented by adding the steric stabilizers like poly(vinyl alcohol), poly(N-vinylpyrrolidone) and cellulose ethers etc. However, in the present system, the bulky surfactant like DBSA also acts as a steric stabilizer and prevents the occurrence of any macroscopic precipitation.

The FTIR transmittance spectra (Fig. 3) of all PANI samples viz. PDB, PCD, PLS and PCS display distinct bands in the range 1550-1570 cm^{-1} and 1475-1495 cm^{-1} due to C=C stretch mode of quinoid diimine (N=Q=N) and benzenoid diamine (N-B-N) segments[27,35], which confirmed the formation of PANI. In addition, bands around 1002-1005 and 1020-1030 cm^{-1} were identified as symmetric and asymmetric stretching vibrations of the –S=O bonds of the dopant counter-anions and 870-885 cm^{-1} bands represent out-of-plane H-C-H bending vibrations of 1,4 di-substituted benzene rings, which confirmed the *para*-coupling of aniline units.

Furthermore, all samples give a band in the range 1146-1152 cm^{-1} which is generally, related to the degree of doping and extent of charge delocalization (or conjugation) over polymer chain, as its intensity gets significantly reduced in the respective undoped/base forms[27]. A careful comparison of normalized intensity of this band gives a qualitative idea about the achieved doping level and in-situ doping capability of used dopants. The above ratio was found to be highest in PDB and it decreased in the order: PDB>PCS>PLS>PCD. This showed that DBSA exert strongest protonation effect on PANI and proved out as the best dopant in comparison to other three sulfonic acids.

The XRD patterns of doped samples (Fig. 4) display characteristic peaks located at 2θ values of ~20° and ~25° that corresponds to periodicity parallel and perpendicular to the chain axis and are characteristic of doped form of polyaniline[25,27,35] (i.e. emeraldine salt). It was also observed that with change in the nature of dopant i.e. PDB (Fig. 2a), PCS (Fig. 4b), PLS (Fig. 4c) and PCD (Fig. 4d), the intensity of 2θ =20° peak decreases whereas that of 25° peak increases, indicating that the doping level decreases in the order PCD>PLS>PCS>PDB.

Figure 5(a) shows that absorption spectra of all the undoped samples of the PANI synthesized in the presence of different sulfonic acid dopants, which exhibit two prominent bands. The first absorption at 320-330 nm (Peak-I) was ascribed to the $\pi_B \rightarrow \pi_B^*$ (or band gap) transition of benzenoid units and its position is directly related to the extent of conjugation. On the other hand, the band near 630 nm (Peak-II) is due to the molecular exciton associated with the quinine–diimine structure i.e., transition of electrons from HOMO orbitals of benzenoid rings and LUMO orbitals of the quinoid rings[25,35] ($\pi_B \rightarrow \pi_Q^*$ transition).

Depending upon the nature of dopant (used during in-situ synthesis), a systematic shift in the position and intensity of absorption maxima of these peaks are observed. In particular, a hypsochromic shift was observed in the position of band-gap transition (Fig. 5a) which signifies reduction of effective

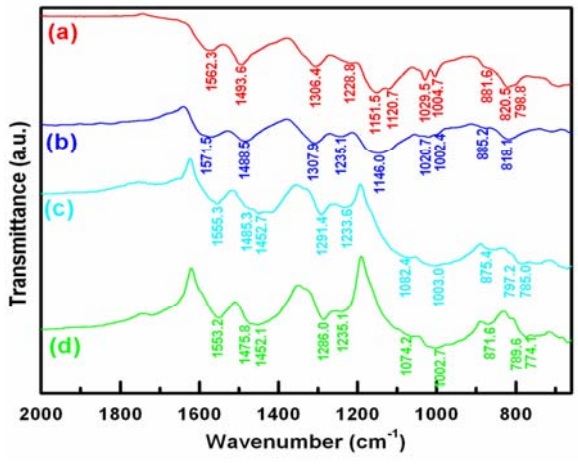

Fig. 3 — FTIR spectra of different bulky organic sulfonic acid doped PANI samples (a) PCD, (b) PDB, (c) PLS and (d) PCS

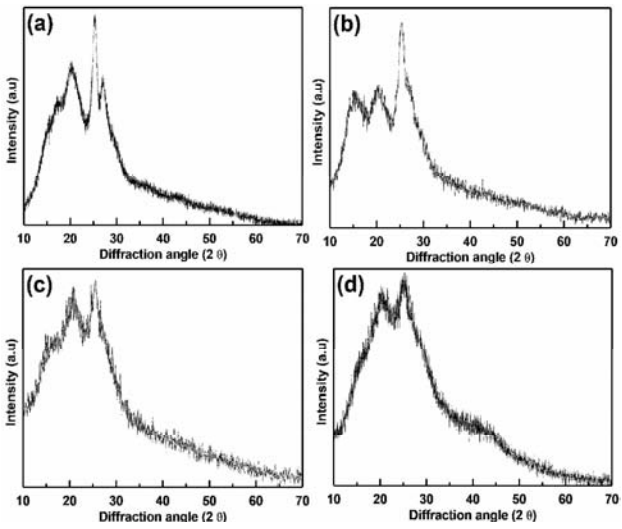

Fig. 4 — XRD patterns of (a) PDB, (b) PCS, (c) PLS and (d) PCD

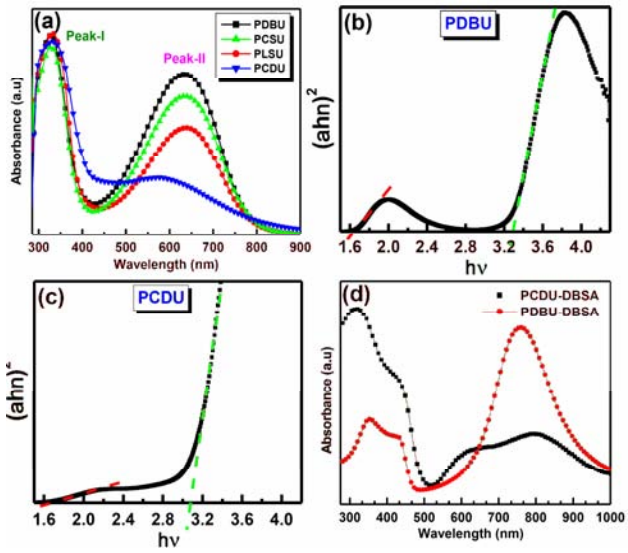

Fig. 5 — UV/Visible spectra of (a) base forms of samples viz. PCDU, PLSU, PCSU, PDBU in NMP; $(\alpha h\nu)^2$ versus hν plots for (b) PDBU & (c) PDBU and (d) spectra of DBSA redoped forms of the PDBU & PCDU in chloroform

conjugation. In addition, a hypsochromic shift and decrement in the intensity of the exciton band were also observed, suggesting a shift towards more reduced state i.e. towards lower oxidation state (OS). The band gap energies of the conducting polymers are closely related to their OS and doping level and often lies in the UV-Visible region. Further, the band-gap of an amorphous semiconducting material can be expressed by following generalized Tauc relation[35,51,1,52]:

$$\alpha h\nu = A(h\nu - E_g)^n \qquad \ldots(1)$$

where α is the absorption coefficient (extinction coefficient), 'hν' is the energy of incident photons of frequency 'ν', E_g is optical band gap and 'A' is a constant of proportionality which depends on temperature and can be related to degree of randomness. The exponent 'n' is related to the distribution of density of states within 'k-space' and assumes values of 1/2, 3/2, 2 and 3 direct allowed, direct forbidden, indirect allowed and indirect forbidden transitions, respectively.

Therefore, for a direct band-gap semiconductor like undoped PANI (EB), the energy associated with the $\pi_B \rightarrow \pi_B^*$ optical absorption edge can be obtained using the expression:

$$\alpha h\nu = A(h\nu - E_g)^{1/2} \qquad \ldots(2)$$

The intersection of the extrapolated tangent drawn on the linear portion of $(\alpha h\nu)^2$ versus $h\nu$ plot, with the x-axis gives value of band-gap (E_g). The calculated results shown in Fig. 5(b and c) revealed that the band gap decreases in the order PDBU>PCSU>PLSU> PCDU, which reflects a shift towards more reduced form.

To investigate further, a careful comparison of absorbance of band-gap (Peak-I) and exciton transitions (Peak-II) was also made, that can give a qualitative estimate of oxidation state[27,35] (OS) [i.e. quantity $(1-y)$] as:

$$(1-y) = \frac{1}{(r+1)} \qquad \ldots(3)$$

where $r = \dfrac{\text{Abs.}[(\text{Peak - I})]}{\text{Abs.}[(\text{Peak - II})]} = \dfrac{[\text{B}]}{[\text{Q}]}$

The calculations show that oxidation state (OS) was the highest in case of PDBU decreases in order PCSU>PLSU>PCDU. These results revealed that PDBU contains nearly equal number of PCDU 'B' and 'Q' units whereas PCDU possess more 'B' units than 'Q' units. Thus, PDB is expected to present in higher doped state than PCD.

Further, all the undoped samples were redoped with DBSA rendering them soluble in chloroform and their absorption spectra was recorded. Fig. 5(d) shows the comparison of the optical spectra of redoped PDBU and PCDU samples. It has been found that doping generates the characteristic bands of protonated emeraldine marked by the presence of three distinct features. The first absorption around 330-360 nm was ascribed to combined effect of $\pi_B \rightarrow \pi_B^*$ (or band gap) transition of benzenoid units plus transition from low lying π_B levels to semi-quinoid or polaron level (π_S), that are formed due to doping of imine (quinoid) nitrogen atoms. On the other hand, the absorption around 420-440 nm ($\pi_S \rightarrow \pi_B^*$) and 700-800 nm ($\pi_B \rightarrow \pi_S$) is related to the polaronic states[27,35]. The absorbance of these polaronic transitions relative to band-gap transitions can be used for qualitative estimation of polaronic content and hence achieved doping level i.e. quantity (x) as:

$$x = \left\{ \frac{Abs.[(\pi_S \rightarrow \pi_B^*) + (\pi_B \rightarrow \pi_S)]}{Abs.[(\pi \rightarrow \pi^*)]} \right\} \qquad \ldots(4)$$

The calculated value of doping level (x) was found to be higher in case of PCDU-DBSA and lowest for

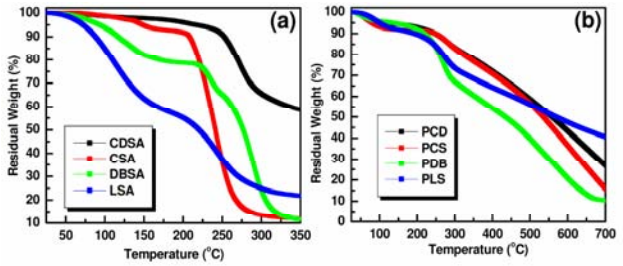

Fig. 6 — TGA plots of (a) dopants and (b) doped PANI samples showing thermal stability range

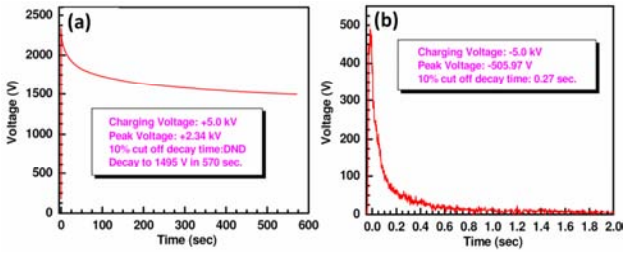

Fig. 7 — Static charge decay profiles of (a) LDPE and (b) PDB/LDPE melt blended film

PDBU-DBSA again suggesting that PDB has more doping centers ('Q' units) than PCD. The electrical conductivity of PCD, PLS, PCS and PDB was found to be 0.73, 1.27, 1.85 and 2.11 S/cm, respectively. This is in accordance with above doping level trend and signifies the importance of dopant on the *E*g, OS, *x* and hence charge transport properties of the doped PANI system.

The TG traces of the pure dopants (Fig. 6a) revealed that CDSA had the highest thermal stability (255°C) whereas LSA (235°C) was least stable. The stabilities of CSA and DBSA were found to 240 and 245°C, respectively. All samples have thermal stability in excess of 230°C, making melt processing theoretically feasible. Figure 6(b) shows the TG traces of the polymers in-situ doped with above polymers. The results revealed that PCD and PCS have IDT value of ~240°C, whereas the PDB and PLS possess IDT values around 235°C. These IDT values were around the melt processing temperatures of conventional thermoplastics like polyethylene (150-160°C) or polypropylene (210-220°C), which suggest that these materials could be processed via melt blended route.

The antistatic performance of blended films was measured using JCI static charge decay test unit where the samples are charged by applying a corona voltage of 5000 V and recording the time required for decay to 10% of accepted voltage. This time is known as 10% cut-off limit and the corresponding 50% discharge time is referred as 50% cut-off limits. The antistatic material suitable for any commercial applications should show 10% cut-off decay time[13,16,17,53,54] of less than 2.0 s. The static charge decay profiles of pure LDPE and PDB/LDPE polyblend are shown in Fig. 7.

The results revealed that when a positive corona potential of 5.0 kV was applied, LDPE accepted as shown in Fig. 7(a), only a fraction of charge corresponding to 2.34 kV of surface voltage. The relatively high value of received voltage can be attributed to the inherently electrically insulating ($\sigma \sim 10^{-16}$ S/cm) nature of LDPE. Further, the transferred charges, tend to stay over the LDPE surface and failed to reach 10% cut-off time limit, even after 500 s. However, incorporation of PDB within LDPE matrix resulted in formation of conducting polyblend with simultaneous improvement of bulk conductivity as well as static charge dissipation rates. Therefore, 1.5% PDB loaded LDPE blend yields decay time of only 0.26 s (Fig. 7b) which clearly passes the antistatic criteria of discharge to 10% of accepted voltage within 2.0 s.

4 Conclusions

Processable PANIs were successfully synthesized by in-situ emulsion polymerization route in the presence of different bulky sulfonic acids which act as surfactant as well as dopant. The formation of PANIs and their successful doping by the above acids was confirmed by FTIR, XRD and UV-Visible measurements. It was observed that oxidation state, doping level and electrical/thermal properties of formed polymers were rationally linked with the nature of dopant. The results also demonstrate superiority of DBSA among other dopants in terms of electrical conductivity, thermal stability and melt procesability. The good thermal stability (>230°C) of these polymers ensures that they can be blended with thermoplastics via melt blending route. Interestingly, melt blended of only 1.5 wt% of PDB with LDPE yields antistatic blend with 10% discharge time of 0.26 s which conforms to antistatic requirement of decay within 2.0 s.

Acknowledgement

Authors wish to thank Director CSIR-NPL for according permission to publish results. Authors also thank Dr. N. Vijayan of NPL for XRD patterns and in charge polymer processing lab, CPSE, IIT Delhi for extending twin screw extruder facility.

References

1 Saini P & Arora M, *New Polymers for Special Appli* (2012) Intech Croatia.
2 Heeger A J, *Angew Chem Intern*, 40 (2001) 2591.
3 Saini P, Arora M, Gupta G, Gupta B K, Singh V N & Choudhary V, *Nanoscale*, 5 (2013) 4330.
4 Trivedi D C & Nalwa H S, *Organic Conductive Molecules & Polymers*, 2 (1997).
5 Skotheim T A, *Conducting Polymers CRC*, (1986).
6 Saini P & Choudhary V, *J Mater Sci*, 48 (2013) 797.
7 Lakshmi K, John H, Mathew K T, Joseph R & George K E, *Acta Materialia*, 57 (2009) 371.
8 Jung J W, Lee J U & Jo W H, *J Phys Chem C*, 114 (2010) 633.
9 Saini P, Choudhary V, Singh B P, Mathur R B & Dhawan S K, *Mater Chem Phys*, 113 (2009) 919.
10 Saini P, Choudhary V, Singh B P, Mathur R B & Dhawan S K, *Synth Met*, 161 (2011) 1522.
11 Wycisk R, Pozniak R & Pasternak A, *J Electrostat*, 56 (2002) 55.
12 Zhang H, Cao G, Wang Z, Yang Y, Shi Z & Gu Z, *Electrochem Solid State Lett*, 11 (2008) 223.
13 Saini P, Choudhary V, Vijayan N & Kotnala R K, *J Phys Chem C*, 116 (2012) 13403.
14 Bai H & Shi G, *Sensors*, 7 (2007) 267.
15 Saini P, Choudhary V & Dhawan S K, *Ind J Engg Mater Sci*, 14 (2007) 436.
16 Saini P & Choudhary P, *J Nanoparticle Resea*, 15 (2013) 1415.
17 Saini P & Choudhary P, *Ind J Pure Appl Phys*, 51 (2013) 112.
18 Mattosso L H C, Faria R M, Bulhoes L O S, Mac Diarmid A G & Epstein A J, *J Polym Sci A, Polym Chem*, 32 (1994) 2147.
19 Rosner R B, *IEEE Trans Device Mater Reliab*, 11 (2001) 86.
20 Reinhold V N & Edenbaum J, *Plastics Additives & Modifiers*, (1992).
21 Narkis M, Lidor G, Vaxman A & Zuri L, *J Electrostat*, 47 (1999) 201.
22 Li C, Liang T, Lu W, Tang C, Hu X, Cao M & Liang J, *Comp Sci Tech*, 64 (2004) 2089.
23 Pikovskaya O G, Derbeneva T E, Panova L N, Chaplanov P E, Merkotun Z Y & Polkovnichenko I T, *Fiber Chem*, 12 (1981) 295.
24 Li Y J, Xu M, Feng J Q & Dang Z M, *Appl Phys Lett*, 89 (2006) 072902.
25 Kobayashi T, Wood B A, Takemura A & Ono H, *J Electrostat*, 64 (2006) 377.
26 Saini P, Choudhary V, Dhawan S K, *J Appl Polym Sci*, 23 (2012) 343.
27 Yukishige H, Koshima Y, Tanisho H, Kohara T, *US patent*, 5,571 (1996) 859.
28 Saini P, Jalan R, Dhawan S K, *J Appl Polym Sci*, 108 (2008) 1437.
29 Dao L H, Leclerc M, Guay J & Chevalier J W, *Synth Met*, 29 (1989) 377.
30 Mattosso L H C, Faria R M, Bulhoes L O S, Mac Diarmid A G & Epstein A J, *J Polym Sci A, Polym Chem*, 32 (1994) 2147.
31 Savitha P, Rao P S & Sathyanarayana D N, *Polym Int*, 54 (2005) 1243.
32 Cao Y, Smith P & Heeger A J, *Synth Met*, 48 (1992) 91.
33 Wessling B, *Synth Met*, 102 (1999) 1396.
34 Chen S A & Lin L C, *Macromol*, 28 (1995) 1239.
35 Saini P & Arora M, *J Mater Chem A*, 1 (2013) 8926.
36 Saini P, Choudhary V, Sood K N & Dhawan S K, *J Appl Polym Sci*, 113 (2009) 31465.
37 Brazovskii S A & Kirova N N, *Sov Phys Lett*, 33 (1981) 4.
38 Heeger A J, *TRIP*, 3 (1995) 39.
39 Huang W-S, Mac Diarmid A G & Epstein A J, *J Chem Soc, Chem Commun*, (1987) 1784.
40 Gowarikar V R, Viswanathan N V, Sreedhar J, *Polymer Science*, (2003).
41 Odian G G, *Principles of Polymerization*, (2004) Wiley-Interscience.
42 Gilbert R G & Naper G H, *J Chem Soc Faraday I*, 71 (1974) 391.
43 Huang H L & Lee W M G, *Chemoshere*, 44 (2001) 963.
44 Smith W V & Ewart R W, *J Chem Phys*, 16 (1948) 592.
45 CapekvIv, Stud Interphse Sci, 23 (2006) 71.
46 Kim B-J, Oh S-G, Han M-G & Kim S-S, *Synth Met*, 122 (2001) 297.
47 Haba Y, Segal E, Narkis M, Titelman G I & Siegmann A, *Synth Met*, 110 (2000) 189.
48 Han M G, Cho S K, Oh S G & Im S S, *Synth Met*, 126 (2002) 53.
49 Kobayashi T, Yoneyama H & Tamura H, *J Electroanal Chem*, 161 (1984) 419.
50 Kobayashi T, Yoneyama H & Tamura H, *J Electroanal Chem*, 177 (1984) 281.
51 Han D, Chu Y, Yang L, Liu Y & Lv Z, *Colloids Surfac*, 259 (2005) 179.
52 Tauc J, *Mater Resea Bull*, 3 (1968) 37.
53 Saini P & Choudhary V, *J Appl Polym Sci*, 129 (2013) 2832.
54 Chubb J N, *J Electrostat*, 65 (2007) 607.